AGU PUBLICATIONS

JGR

Journal of Geophysical Research: Space Physics

RESEARCH ARTICLE
10.1002/2014JA020914

Key Points:
- Polar cap patches populate both the dawn and the dusk cells symmetrically
- The symmetry in patch exits at night is marginally affected by IMF B_y
- East-west elongated patches are torn apart when grabbed by tail reconnection

Supporting Information:
- Movie S1

Correspondence to:
J. Moen,
jmoen@fys.uio.no

Citation:
Moen, J., K. Hosokawa, N. Gulbrandsen, and L. B. N. Clausen (2015), On the symmetry of ionospheric polar cap patch exits around magnetic midnight, *J. Geophys. Res. Space Physics*, *120*, 7785–7797, doi:10.1002/2014JA020914.

Received 14 DEC 2014
Accepted 9 JUL 2015
Accepted article online 14 JUL 2015
Published online 4 SEP 2015

On the symmetry of ionospheric polar cap patch exits around magnetic midnight

J. Moen[1], K. Hosokawa[2], N. Gulbrandsen[3], and L. B. N. Clausen[1]

[1]Department of Physics, University of Oslo, Oslo, Norway, [2]Department of Communication Engineering and Informatics, University of Electro-Communications, Tokyo, Japan, [3]Department of Physics and Technology, University of Tromsø, Tromsø, Norway

Abstract In this paper we examine how polar cap patches, which have been frozen into the antisolar flow over the polar cap, are transported into the nighttime auroral oval. First we present a detailed case study from 12 January 2002, with continuous observations of polar cap patches exiting into the nighttime auroral oval in the Scandinavian sector. Satellite images of the auroral oval and all-sky camera observations of 630.0 nm airglow patches are superimposed onto Super Dual Auroral Radar Network convection maps. These composite plots reveal that polar cap patches exit on both the dusk and on the dawn convection cells. Then we present statistics based on 8 years of data from the meridian scanning photometer at Ny-Aalesund, Svalbard, to investigate the possible interplanetary magnetic field (IMF) B_y influence on the distribution of patch exits around magnetic midnight. The magnetic local time distribution of patch exits is almost symmetric around magnetic midnight, independent of IMF B_y polarity. Synthesizing these observations with previous results, we propose a three-step mechanism for why patch material exits symmetrically around midnight. First, intake of patch material occurs on both convection cells for both IMF B_y polarities. Second, plasma intake by transient magnetopause reconnection stretches the newly cut polar cap patches into dawn-dusk elongated forms during their transport into the polar cap. And finally at exit, dawn-dusk elongated patches are split and diverted toward both the dawn and dusk flanks when grabbed by transient tail reconnection.

1. Introduction

Polar cap patches in the *F* region ionosphere are defined as islands of elevated electron density (factor of 2 or more above the background [*Crowley*, 1996]). *Foster* [1984] mapped the intake of solar EUV-ionized plasma through the cusp inflow region to be 3–4 h wide around magnetic noon. The subsequent transport of high-density plasma across the polar cap from day to night has now been well documented [*Foster et al*., 2005; *Hosokawa et al*., 2009c, 2010b; *Zhang et al*., 2013a]. The polar cap patch phenomenon is regarded as a challenging space weather issue [e.g., *Spogli et al*., 2009; *Prikryl et al*., 2010, 2011; *Moen et al*., 2013] because the electron density gradients associated with polar cap patches give rise to disturbances on HF radio communication links and may under extreme conditions give rise to inaccuracy or loss of signals in satellite navigation and communication systems. In order to provide regional forecasts of, for example, radio wave scintillations to the user community, it will be necessary to know exactly how high-density solar EUV-ionized plasma is entrained in the polar cap convection flow around noon and then populates the convection cells. We also need to improve our knowledge about the polar cap flow dynamics while the patches are in transport across the polar cap from day to night. And finally, we need to know exactly how polar cap patches exit into the aural oval around magnetic midnight. The main objective of this paper is to present new insights about patch exits around midnight. We will present continuous observations of a train of polar cap patches that exited the polar cap during a 6 h period in the Scandinavian Arctic sector on 12 January 2002. We will also present a statistical study of the possible interplanetary magnetic field (IMF) B_y influence on the magnetic local time (MLT) distribution of patch exits. In order to provide a proper background to discuss our observations we will first give a brief introduction to established knowledge on (i) intake of patch material, (ii) patch transport across the polar cap, and (iii) patch exiting the polar cap. Throughout this paper we use the term open-closed boundary (OCB), i.e., the boundary between open and closed field lines, as an equivalent to polar cap boundary [*Siscoe and Huang*, 1985].

1.1. Intake of Patch Material

Buchau et al. [1983] and *Weber et al*. [1984] undertook pioneering work with high-sensitivity all-sky imagers to monitor patch dynamics in detail and found the polar cap to be filled with patches during IMF B_z negative

conditions. It was noticed that the patch forms are often strongly elongated oval forms, and they introduced the descriptive term "cigar-shaped" patches (cf. Figure 7 in *Carlson* [2003]). Recently, *Hosokawa et al*. [2014] visualized such cigar-shaped patches by using two all-sky airglow imagers in the polar cap region. They have shown that the dawn-dusk extent of the patches was as large as 2000 km while the thickness in the direction of their motion was only about 500 km. These previous studies indicate that the typical shape of polar cap patches during nonstorm time intervals is cigar shaped. Several mechanisms have been proposed to explain how cusp reconnection dynamics can explain segmentation of the tongue of ionization into patches and most of them are related to the dynamics of transient reconnection and includes polar cap boundary motions, current sheets, and flow channels [cf. *Anderson et al*., 1988; *Lockwood and Carlson*, 1992; *Rodger et al*., 1994; *Milan et al*., 2002; *Rodger et al*., 1994; *Sojka et al*., 1993; *Valladares et al*., 1994; *Pitout and Blelly*, 2003; *Pitout et al*., 2004; *Carlson et al*., 2004; *Lockwood et al*., 2005; *Moen et al*., 2006; *Carlson et al*., 2004, and references therein]. *Lockwood and Carlson* [1992] provided a model for patch formation in the cusp inflow region by pulsed reconnection which could explain the cigar-shaped patch forms. (This is illustrated in Figures 8a and 8b in the Discussion section).

There are only a few detailed documentations of how solar EUV-ionized plasma enters the convection cells from subauroral latitudes. *Zhang et al*. [2011] demonstrated that patch formation may be sensitive to IMF $|B_y|$. It has been demonstrated that variability in the IMF B_y strength can regulate patch structuring [e.g., *Zhang et al*., 2011; *Sakai et al*., 2013]. *Oksavik et al*. [2010] traced a polar cap patch back to its probable entry region in the dusk cell during IMF B_y positive condition. To our knowledge, *Zhang et al*. [2013b] presented the first clear documentation of patch entry onto the morning convection cell during IMF B_y negative condition. A statistical analysis by *Moen et al*. [2008] documented that solar EUV-ionized patch material is pulled into the polar cap for both positive and negative polarities of IMF B_y. They revealed an apparent prenoon-postnoon asymmetry in the occurrence rate of high-density patch material consistent with the IMF B_y control of the plasma convection around noon [e.g., *Heppner and Maynard*, 1987; *Ruohoniemi and Greenwald*, 2005]. In summary, according to present knowledge, solar EUV-ionized plasma may enter the polar cap for both polarities of IMF B_y.

1.2. Patch Transport Across the Polar Cap

Polar cap patches are frozen into the plasma convection, and their actual flow path across the polar cap path is controlled by the IMF conditions [*Cannon et al*., 1991; *Fukui et al*., 1994; *Hosokawa et al*., 2006]. *McEwen and Harris* [1996] and *Zhang et al*. [2003] documented an IMF B_y control on azimuthal motion of the patches observed at Eureka station, ideally situated in the middle of the polar cap at Eureka (89° corrected geomagnetic latitude (CGM)), Canada, consistent with convection models developed by *Weimer* [1995] and *Hairston and Heelis* [1990]. *Hosokawa et al*. [2009b] presented similar statistical results by applying automated patch detection and velocity determination procedures to all-sky airglow imager observations at Resolute Bay (83° CGM). Several convection streamline techniques have been developed and successfully applied to connect patch motion observed by localized measurements [*Pedersen et al*., 2000; *Crowley et al*., 2000; *Bust and Crowley*, 2007; *Oksavik et al*., 2010]. *Oksavik et al*. [2010] based their technique on 2 min resolution Super Dual Auroral Radar Network (SuperDARN) convection maps and found that the movement was pulsed, consistent with the *Cowley and Lockwood*'s [1992] convection model description of transient reconnection. *Hosokawa et al*. [2013] demonstrated an existence of mesoscale structure embedded in large-scale patches, which may be caused by the pulsed nature of the patch production and transportation process as suggested by *Oksavik et al*. [2010]. *Oksavik et al*. [2010] also pointed out that the first patch into the polar cap would not necessarily have to be the first one exiting the polar cap. This sort of complex behavior of patches during their travel across the polar cap was also pointed out by *Hosokawa et al*. [2010a], who showed a case in which a patch traveling in the central polar cap region was split into two parts by the shear in the background plasma convection.

1.3. Patch Exiting the Polar Cap

When polar cap patches exit the polar cap into the auroral oval they are degraded and form a wedge of auroral blobs [*Robinson et al*., 1985; *Crowley et al*., 2000]. Detailed observations have been carried out by using radar and optics to study the transition from patch to auroral blob structure [*Crowley et al*., 2000; *Wood et al*., 2009]. *Lorentzen et al*. [2004] presented high-resolution observations of how a sequence of polar cap

patches is drawn into the auroral oval during episodes of tail reconnection. *Crowley et al*. [2000] and *Bust and Crowley* [2007] reported that patches turning into blobs may straddle the return flows toward the dayside on the dawn cell and the dusk cell. *Moen et al*. [2007] presented the MLT distribution of patch exits observed by a meridian scanning photometer operated at Ny-Aalesund, Svalbard, using 8 years of observations. They found that the patch exit distribution function was a bell-shaped function peaking at 23:30 MLT, indicating that polar cap patches may exit the polar cap on both convection cells. They did not, however, study the influence of the IMF B_y component on this distribution.

The main objective of the current paper is to study if there is any IMF B_y regulation of polar cap patch exits at night. The paper is organized as follows: in section 2 we will describe the instrumentation used. In section 3 we will present synthesized SuperDARN HF radar observations, IMAGE/FUV images of the large-scale auroral oval, and all-sky 630.0 nm airglow observations of polar cap patch exits around magnetic midnight. This excellent data set is from 12 January 2002. Thereafter, we present a reanalysis of the statistical data set used by *Moen et al*. [2007] to check if there is any IMF B_y effect on the patch exits. This is followed by the discussion in section 4 and then summary and conclusions in section 5.

2. Instrumentation

For the interplanetary magnetic field (IMF) and solar wind plasma conditions we use observations from the ACE spacecraft [*Chiu et al*., 1998] located near the L1 point. In this paper we will present data from the magnetic field experiment [*Smith et al*., 1998], and we are using plasma measurements from the Solar Wind Electron Proton Alpha Monitor [*McComas et al*., 1998] to estimate the time delay from the ACE location to the magnetopause.

The polar cap patches are monitored by the University of Oslo's optical instruments located at Ny-Aalesund, Svalbard (78.92°N, 11.93°E; 76° magnetic latitude; 24:00 MLT = 20:50 UT). It comprises a meridian scanning photometer (MSP) and an all-sky CCD imaging system. The meridian scanning photometer swept the magnetic meridian from north to south at ~20 s resolution. The instrument operates at four wavelengths: 630.0 nm (OI), 557.7 nm (OI), 427.8 nm (N_2^+ 1NG), and 486.1 nm (H_β). The all-sky imager acquired six images per minute, one 630.0 nm image every 30 s followed by two 557.7 nm images. The exposure time was 1 s for the 630.0 nm wavelength and 0.5 s for the 557.7 nm wavelength. As this paper focuses on 630.0 nm airglow patches we are going to present observations from the 630.0 emission line for both instruments.

The large-scale auroral context for the polar cap patches observed from ground is provided by the far ultraviolet wideband imaging camera (FUV/WIC) instrument [*Mende et al*., 2000a, 2000b] on board the Imager for Magnetopause-to-Aurora Global Exploration (IMAGE) satellite. FUV/WIC is sensitive to auroral emissions over a broad range of the UV spectrum (140–160 nm), the primary component of which is associated with precipitating electrons. The spin of the IMAGE spacecraft was such that images were captured with a cadence of 2 min. During the interval shown in this study, IMAGE was located near apogee in the northern hemisphere, and the distance from the spacecraft to the center of the Earth was ~7–8 R_E. This enables us to monitor the entire distribution of the northern auroral oval throughout the interval.

The high-latitude convection maps presented in this study were derived from the coherent HF radars of Super Dual Auroral Radar Network (SuperDARN) [*Chisham et al*., 2007] in the northern hemisphere using the map-potential technique developed by *Ruohoniemi and Baker* [1998]. The radars of SuperDARN are capable of detecting backscatter from plasma irregularities at *F* region heights that are generated by plasma instabilities. Patches are known to be one of the sources of *F* region irregularities [e.g., *Basu et al*., 1990; *Milan et al*., 2002; *Mitchell et al*., 2005; *Hosokawa et al*., 2009a; *Carlson et al*., 2007; *Moen et al*., 2013; *Jin et al*., 2014]; thus, during the current interval, we obtained some radar echoes from patches themselves. Because these irregularities tend to drift at the background plasma velocity, the line-of-sight component of ionospheric convection is measurable by examining the obtained Doppler spectra. When we derived the convection maps, the data from eight radars in the northern hemisphere were projected onto the 400 km altitude plane and integrated in 2 min intervals; thus, the temporal resolution of the map is 2 min.

We also show measurements of the total electron content (TEC) along a signal path from a GPS satellite to the ground receiver station. These TEC values were obtained from the Madrigal database and are estimated using data from a global network of GPS receivers, mapped from the line of sight to the vertical direction, and

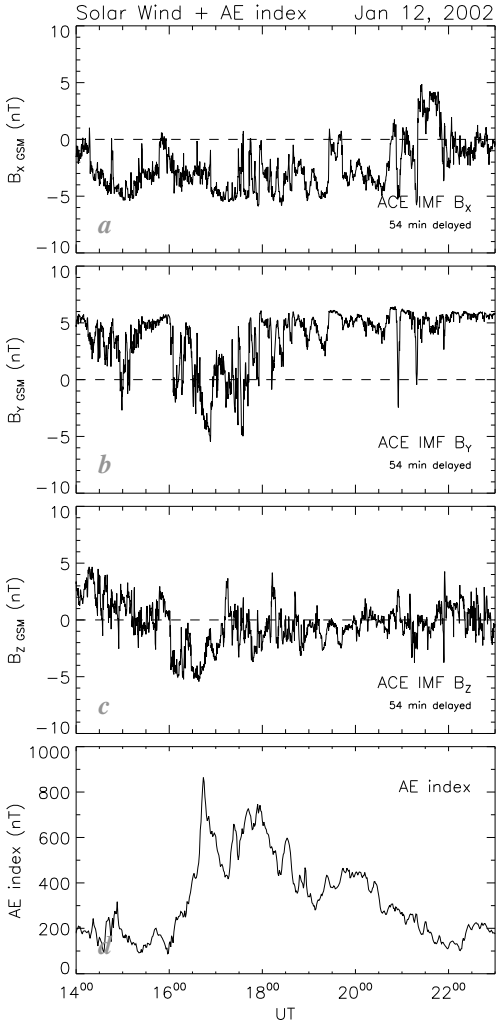

Figure 1. (a–c) The three components of the interplanetary magnetic field from the ACE satellite are presented in GSM coordinates. The time axes for these data are delayed by 54 min to ease the comparison with ground data. (d) Magnetic *AE* index.

provided in 1°×1° bins every 5 min distributed over those locations where data are available [*Rideout and Coster*, 2006]. To improve the data coverage these data are regridded onto a 2°×2° grid. In this paper we are using the TEC value as a proxy for the ionospheric plasma density since it is in the ionospheric plasma that polar cap patches manifest themselves. While the ionospheric plasma is the biggest contributor to the TEC value, it is important to note that other parts of the magnetosphere at higher altitudes also contribute. *Makarevich and Nicolls* [2013] have shown that sources above 660 km altitude can contribute as much as 30% to the TEC value but that on average their contribution is about 20%.

3. Observations

3.1. A Case Study From 12 January 2002

Figures 1a–1c display the IMF recorded by ACE from 14:00 to 23:00 UT on 12 January 2002. The IMF data have been plotted with a delay of 54 min to account for the solar wind travel time from the ACE location to arrival at the dayside magnetopause. The IMF was variable with fluctuations ranging from −5 nT to +5 nT in all three components. IMF B_z was positive until 16:00 UT when there was a sharp southward turning to −4 nT. It then remained negative until 17:20 UT, and thereafter, it was unsettled with alterations between −3 and 3 nT. IMF B_y was predominantly positive except between 16:30 and 17:40 UT when several major negative excursions occurred. The longest-duration B_y negative excursion occurred around ~16:40 UT and lasted for ~20 min. IMF B_x was predominantly negative except for the major positive excursion between 21:20 and 22:00 UT.

Figure 1d presents the corresponding *AE* index which is sensitive to auroral electrojets stimulated by reconnection activity. The *AE* index shows a strong activity enhancement above 200 nT from 16:10 to 21:30 UT. A maximum value of 850 nT was reached around 16:45 UT, which was 45 min after the sharp IMF B_z negative transition. Thereafter, strong modulations occurred on the time scale of 1–3 h, onto which smaller but notable fluctuations occurred on ~10 min time scale.

Figure 2 presents the solar wind forcing of the polar cap in terms of ion flows and intake of solar EUV-ionized plasma in form of a sequence of TEC (total electron content) data acquired by ground GPS receivers superimposed onto SuperDARN convection maps. In 1 h time steps the eight maps cover the entire time interval of interest. High-density solar EUV-ionized plasma (in red) is seen to enter the cusp inflow region in the 16:10 UT picture, when the convection pattern expands equatorward onto the region of high-density solar EUV-ionized plasma. The equatorward expansion of the polar cap is a signature of intensified magnetopause reconnection [*Cowley and Lockwood*, 1992] and is consistent with the sharp negative turning in IMF B_z impinging the magnetopause at 16:00 UT (Figure 1c). This is 2 h prior to the train of patches that we will study exiting the polar cap at night. A significant amount of plasma is seen to populate the dusk return flow in the 19:10 image. Notable plasma intake occurred on both convection cells in the 18:10 and the 19:10 images. At 20:10 UT we see that the high-density plasma exiting around midnight is diverted toward dayside on both convection cells. However, the spatial coverage of GPS TEC data is not sufficient to reveal any detailed

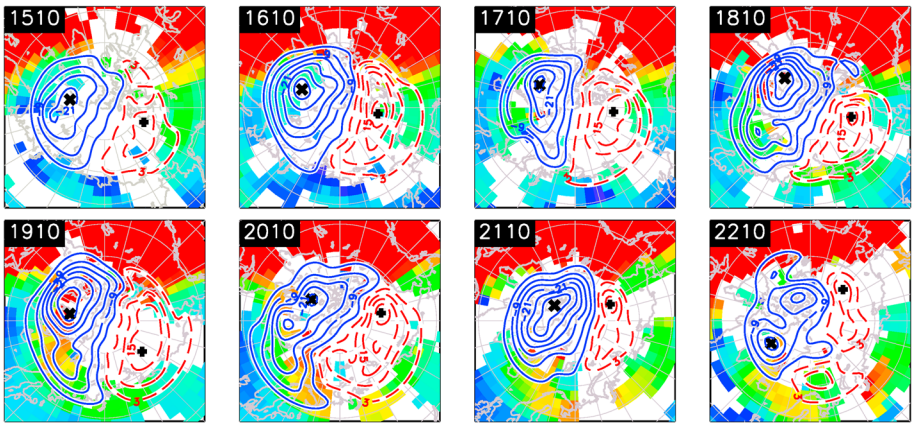

Figure 2. A sequence of TEC maps onto which SuperDARN convection maps have been superimposed. The data coverage and resolution of this map is too coarse to see any details, but it demonstrates that there was patch intake around noon and patch exits around midnight on both convection cells.

dynamics of the high TEC plasma flow. There is an unfortunate data gap in the Russian Arctic sector in the dawn cell exit region (the white region just after magnetic midnight). However, this global view provides useful background information for when we zoom in on patch exit dynamics.

Figure 3a presents a sequence of 630.0 nm airglow patches observed on 12 January 2002 in a keogram format. The 630.0 nm emission intensity is plotted versus scan angle from 15°N to 165°S and universal time from 17:10 to 24:00 UT. Airglow patches drifting along the magnetic meridian from north to south appear as inverted integral signs in the keogram. They appear to spend more time near the horizons which is an artifact of the nonlinear conversion between scan angle and spatial distance. The poleward auroral boundary of the nighttime aurora moved northward around 17:10 UT, and after several intensifications and poleward bounces, the poleward auroral boundary finally receeded equatorward and stopped near the equatorward border of the MSP field of view around 22:05 UT, after which it grew faint and disappeared around 23:20 UT.

The poleward boundary of the substorm aurora is taken as a visible proxy of the open-closed boundary (OCB) [e.g., *Blanchard et al*., 1996; *Ober et al*., 2001; *Østgaard et al*., 2005], and the poleward boundary leap is taken as

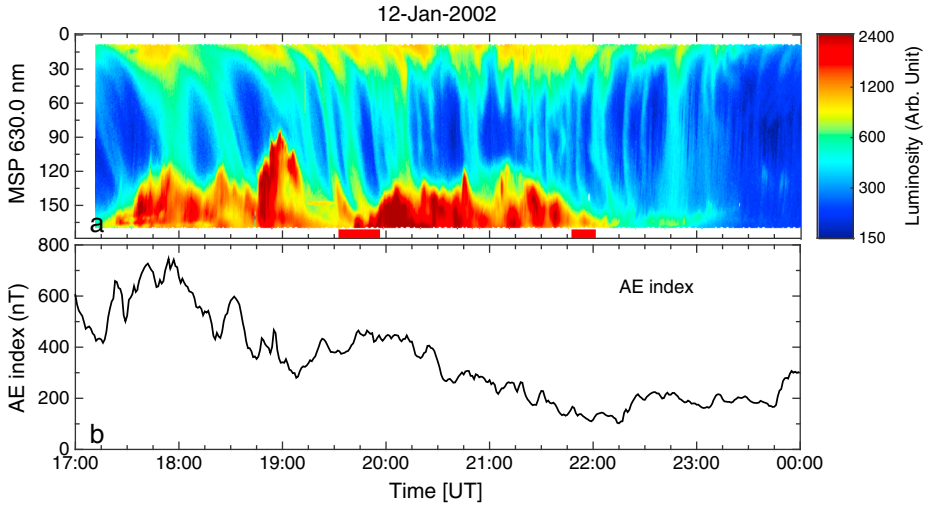

Figure 3. (a) Meridian scanning photometer data from Ny-Aalesund, 12 January 2002, from 17:10 to 24:00 UT as function of scan angle from 15°N to 165°S. The intensity is color coded in log counts. Ny-Aalesund crosses magnetic midnight at 20:50 UT. The traces from north to south are airglow patches. The red bars on the time axis mark the two time intervals covered by all-sky observations in Figures 4, 5. (b) The *AE* index for comparison with the auroral observations. Notably, there is an increase in the *AE* index every time a patch is pulled through the poleward auroral boundary.

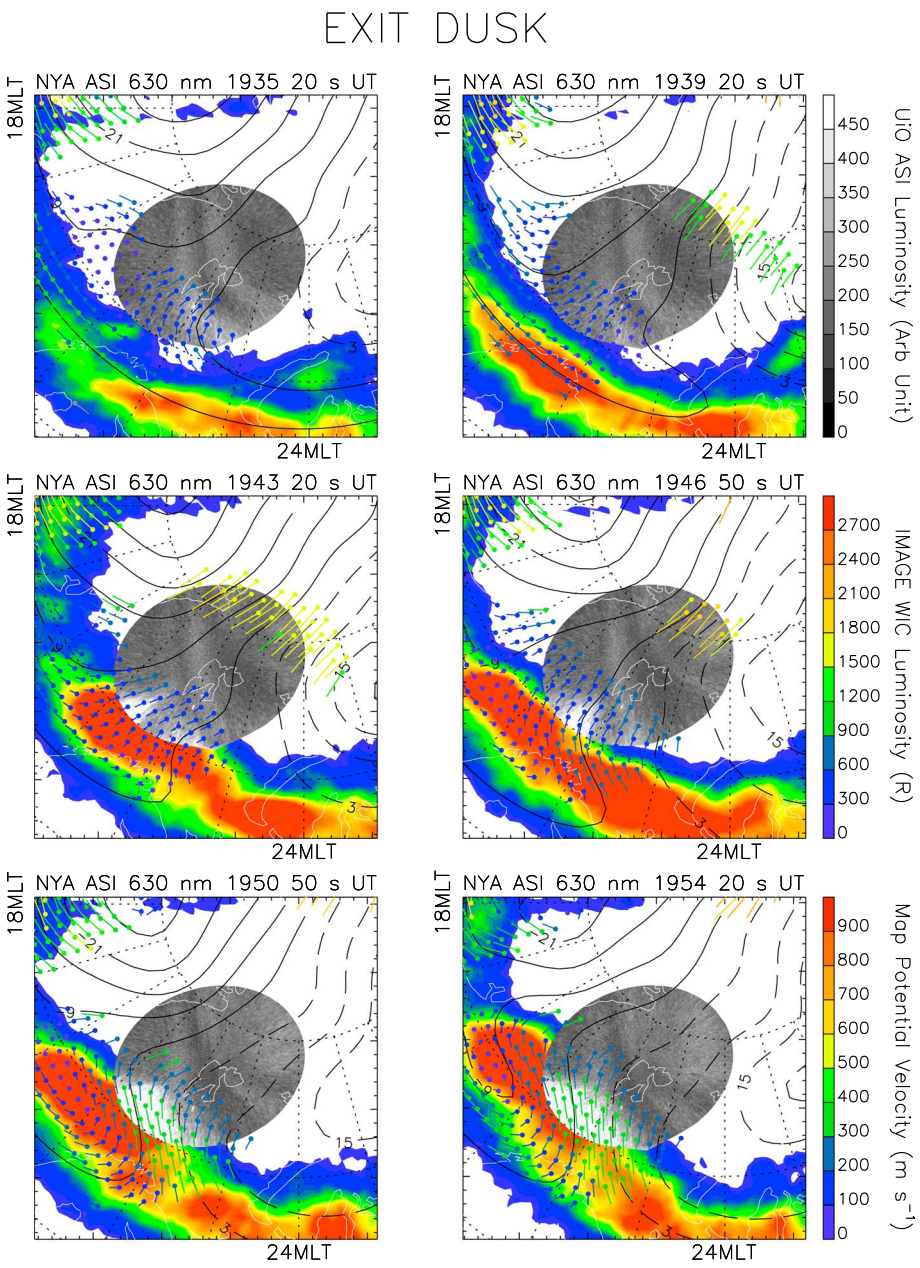

Figure 4. Composite plot of the satellite FUV images (colored), SuperDARN convection pattern, and 630.0 nm all-sky images (grey). (first column) The intensity/color bars for the 630.0 nm all-sky camera are given on the right (counts), (second row) for the IMAGE WIC luminosity, and (third row) for the SuperDARN convection vectors. This figure demonstrates a sequence of cigar-shaped patches that were pulled out of the polar cap onto the dusk convection cell.

a signature of intensified tail reconnection. Every time a 630.0 nm airglow trace hits the auroral boundary and disappears, it indicates that a polar cap patch propagated across the OCB, i.e., exited the polar cap [*Lorentzen et al.*, 2004; *Moen et al.*, 2007]. Notably, there is a good overall correspondence between major poleward leaps and intensifications in the *AE* index, presented in Figure 3b. Looking in more detail, every patch encounter was associated with at least a small perturbation in the *AE* index. This indicates that enhanced nightside reconnection is a prerequisite for patches to enter the auroral oval. On the other hand, intensifications of the *AE* index also occurred without patch signatures; this is sensible since the *AE* index measures the strength of the auroral electrojet and hence nightside reconnection which is not modulated by polar cap patches.

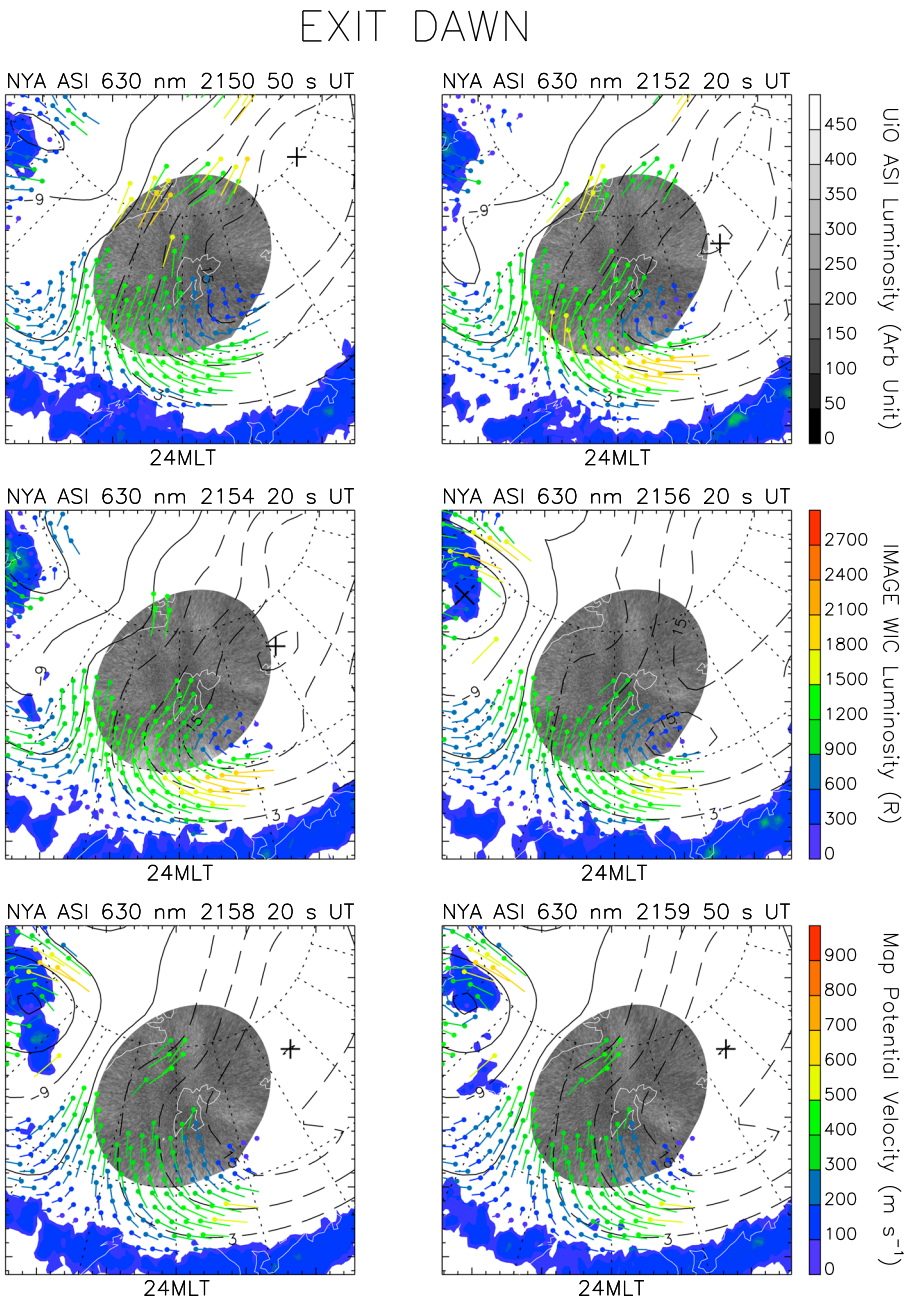

Figure 5. Example of patch exits onto the dawn convection cell presented in the same format as in Figure 4.

Now let us focus on identifying the convection cell that received the polar cap patches when they exited the polar cap. We will demonstrate that the patches observed before 21:20 UT exited on the dusk convection cell and the patches observed after 21:20 UT (00:40 MLT) exited on the dawn convection cell. Figures 4 and 5 present a composite plot of the IMAGE/FUV data in the northern hemisphere auroral oval (colored), SuperDARN convection pattern, and the all-sky camera (grey) that extended optical coverage to include polar cap patches. This data set provides the first direct two-dimensional (2-D) monitoring of how polar cap patches exit the polar cap. Figure 4 shows a sequence of images from 19:35 to 19:54 UT (22:45–23:04 MLT). In the two first images in Figure 4 we see two cigar-shaped patches which in the following images disappear across the auroral boundary on the dusk convection cell. The time interval of this image sequence has been marked with a red bar on the time axis in Figure 3a. Notably, the poleward auroral boundary leapt poleward to grab one patch at a time. The boundary receded equatorward after each leap, indicating relaxation in the reconnection

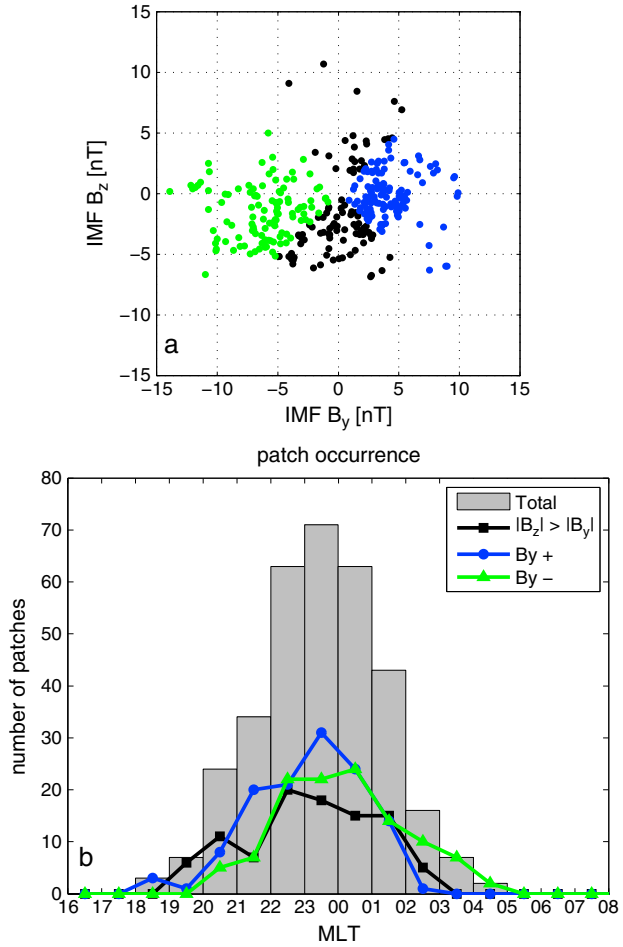

Figure 6. (a) IMF vectors plotted in the GSM *y-z* plane. The patch observations have been sorted by clock angle using the following sectors: B_y+: 45° to 135° in blue, B_y−: 225 to 315° in green, and $|B_z| > |B_y|$ in black. (b) Histogram of polar cap patch pulled out of the polar cap over Ny-Aalesund as a function of MLT (magnetic local time) as presented by *Moen et al*. [2007]. The black, green, and blue curves show the distribution of patch exits for the clock angles defined in the Figure 6a. There is a notable IMF B_y asymmetry on the flanks, but the patch exits are nearly symmetric around midnight.

rate between each patch grabbing. Figure 5 shows a sequence of patches imaged between 21:50 and 21:59 UT on their way to exit on the dawn convection cell. This time interval is marked with a second red bar in Figure 3a, guiding our eye to see the patch signature grabbed around 21:55 UT. The auroral intensity was below the threshold for the UV imager. The MSP, however, could track the poleward boundary until it gradually grew faint and disappeared around 23:20 UT. The airglow patches exiting postmidnight were less intense than those prior to midnight. In order to better visualize the auroral boundary intensifications and patch grabbing we have made a video for the time interval for 17:30–22:50 UT. We strongly recommend that the reader views this video since it is not possible to fully appreciate the patch exit dynamics from still images. When viewing the video, please note how the direction of the patch movement is consistent with the antisunward flow in the polar cap and that the zonal direction may flip near the exit region on the dawn cell, as, e.g., observed in Figure 4 from westward in the 19:43.20 UT frame, to equatorward in the 19:46.50 UT frame, to eastward in the 19:50 UT frame. From the video it is evident that the auroral band after 22:15 UT was comprised of pulsating postnoon auroras. The dawn cell patches were observed from 21:20 UT onward. IMF B_y was strongly positive except for a couple of brief excursions negative around 21:00 UT and 21:20 UT (cf. Figure 1b).

3.2. A Statistical Study of the IMF B_y Influence on Patch Exits

In order to check whether there is a possible IMF B_y effect on the MLT distribution of patch exits we have reanalyzed the data set used by *Moen et al*. [2007]. Their statistics was based on 8 years of data from the

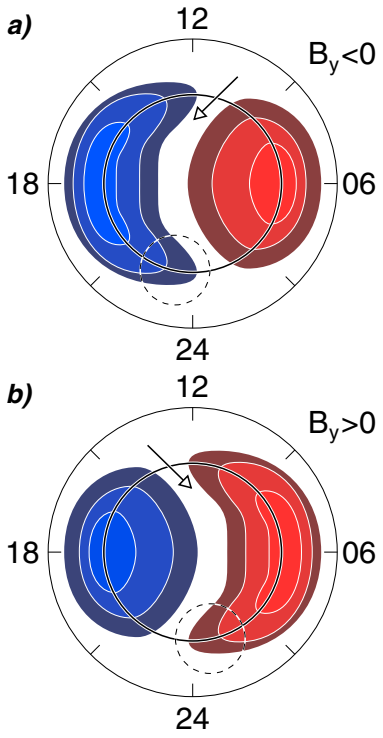

Figure 7. Illustration of the observation geometry. (a) Some of the patches observed to exit polar cap before magnetic midnight entered during IMF B_y negative condition as illustrated on the top. (b) All the patches observed postmidnight must have entered the cusp inflow region during IMF B_y positive condition.

meridian scanning photometer data from Ny-Aalesund. Patch exits were counted every time a patch hit the poleward auroral boundary. For the corresponding IMF conditions we have used ACE solar wind data that have been time shifted from the satellite location around L1 to Earth using constrained minimum variance method (MVAB-0) [*Haaland et al*., 2006; *Sonnerup and Scheible*, 1998; *Weimer and King*, 2008]. In order to determine the IMF condition for a particular patch exit at night, we have chosen to use 30 min averages of the IMF data that preceeded that particular patch exit. This is similar to the averaging used in statistical studies of convection patterns [*Ruohoniemi and Greenwald*, 1996, 2005; *Weimer*, 1995] and was also used in a patch study by *Coley and Heelis* [1998].

The patch OCB crossing was sorted in three IMF clock angle sectors (Figure 6a). Clock angles between 45° and 135° were assigned to B_y+, and clock angles between 225° and 315° were assigned B_y-. The rest was assigned to a category of B_z-dominated IMF ($|B_z| > |B_y|$). From a total number of 333 patch observations, 123 belong to B_y+ and 113 belong to B_y-; i.e., both polarities are equally represented. Figure 6b presents the MLT distributions of patches for the different clock angle categories. The B_y+ is slightly tilted toward premidnight, while the B_y- is slightly tilted toward postmidnight. The average MLT exit for a patch in B_y+ is 23:02 MLT, while for B_y- it is 00:04 MLT. The slight east-west skew in the patch exit distributions corresponds well with a similar skew in the statistical convection patterns around midnight due to IMF as demonstrated by *Ruohoniemi and Greenwald* [2005]. This is also consistent with the fact that the patches are frozen into the $E \times B$ drift, and it indicates that dawn and dusk convection cells are symmetrically populated by patch material independent of the IMF B_y polarity.

4. Discussion

We have presented continuous observations of a sequence of polar cap patches being pulled across the nightside polar cap boundary into the auroral oval during a 5.5 h period around magnetic midnight. The patches were observed to exit the polar cap on the dusk cell premidnight, and on the dawn cell postmidnight, as the optical station rotated underneath the convection system. From the statistics presented in Figure 6b there is no apparent IMF B_y asymmetry found in the occurrence rate of patch exits around midnight.

Moen et al. [2008] demonstrated that solar EUV-ionized patch material enters the polar cap regardless of the IMF B_y polarity, but the trajectory of patch material was found to be strongly B_y dependent. In the classical static picture of the twin-cell polar cap convection as illustrated in Figure 7, one might have expected that there would also be an IMF B_y-controlled dawn-dusk asymmetry also in the patch exits around magnetic midnight, i.e., that there exist a skew toward postmidnight for IMF B_y negative condition (Figure 7a) and a skew toward premidnight exits for IMF B_y positive condition (Figure 7b). However, from the statistics we presented in Figure 6b we find no significant IMF B_y asymmetry in the occurrence rate of patch exits around midnight. This begs the question: Why is that?

First, that fact that the MLT distribution of patch exits is insensitive to IMF B_y indicates that both the dawn and the dusk convection cells are populated with patch material regardless of the IMF polarity. The 20:10 UT image in Figure 2 supports this view; plasma is diverted toward dusk and dawn around midnight. As illustrated in Figure 7, the limited field of view of one all-sky imager makes it impossible to make direct observations of patch exits on both the convection cells simultaneously. Fortunately, the IMF B_y polarity changed during the 12 January 2002 case presented which provides us an opportunity to investigate this further:

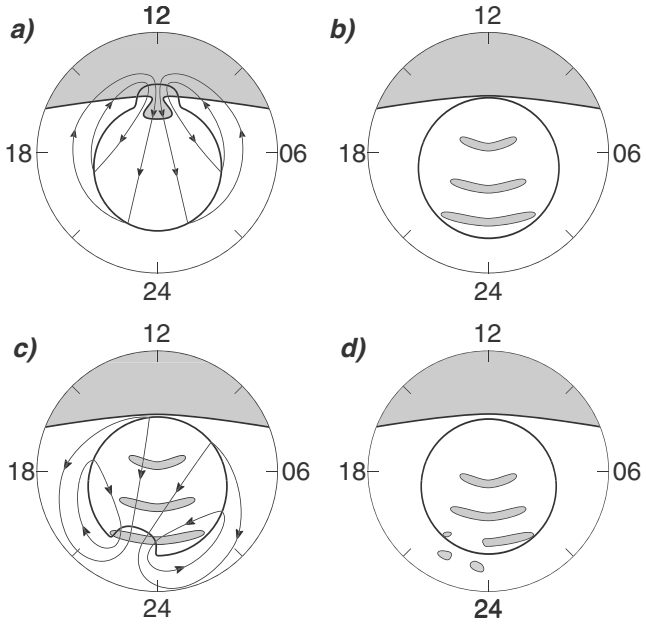

Figure 8. (a and b) Illustrates path stretching due to transient dayside reconnection. (c and d) Illustrates our suggestion how elongated polar cap patches may be torn apart and diverted toward dusk and dawn when exiting the polar cap.

IMF B_y was predominantly positive except between 16:30 and 17:40 UT when several major negative excursions occurred (Figure 1b). The polar cap potential varied between 40 and 70 kV which corresponds to transit times of 2 to 3 h across the polar cap, i.e., from a patch entering the polar cap in the cusp region until it exited the polar cap around midnight. Patches formed during the period of the major IMF B_y negative excursion, between 16:40 and 17:00 UT (Figure 1b), are expected to be those exiting the polar cap from ~19:10 to 19:30 UT ±30 min, i.e., prior to magnetic midnight (22:20–22:40 MLT). The duration of IMF B_y negative condition was not long enough to serve as test. However, the IMF B_y settled into a positive polarity after 17:40 UT, and all the patches observed to exit the polar cap postmidnight (after 21:20 UT = 00:30 MLT) must have been formed when IMF B_y varied between 3 and 5 nT (18:50 UT in Figure 1b). From the observational geometry in Figure 7b for positive IMF B_y, we rather might have expected a preference for patch transport on the dusk cell, if any. Thus, the observed sequence of patch exits on the dawn cell for steady positive IMF B_y strengthens the case that patch transport and patch exits occur on both convection cells simultaneously.

Let us now consider a possible explanation for the IMF B_y-independent symmetry in patch exits around midnight. Figures 8a and 8b illustrate how pulsed reconnection produces a train of east-west elongated patches as originally suggested by *Lockwood and Carlson* [1992]. Figure 8a illustrates how the OCB leaps equatorward to grab solar EUV-ionized plasma (dark grey) during a magnetopause reconnection pulse. The flux transfer event generates a pulse of twin-cell flow that brings high-density plasma on newly opened field lines, across the polar cap boundary, indicated in grey, into the polar cap. The polar cap will expand in the dawn and dusk directions in the case of bursty dayside reconnection as illustrated here [cf. *Cowley and Lockwood*, 1992]. This stretches the patch into a cigar-shaped form which populates both convection cells. Indeed, in our study, many of the patches that arrived at night were cigar shaped (cf. Figure 3a and Movie S1). According to the *Cowley and Lockwood*'s [1992] transient flow model, the duration of an individual flow disturbance is about 15 min, which was experimentally verified by *Moen et al*. [1995]. Therefore, if all reconnection stops, flow-free equilibrium is achieved after 15 min. Figure 8b illustrates three patch forms parked in the polar cap after flow-free equilibrium has been achieved. *Hosokawa et al*. [2011] documented a case where the transpolar movement of a patch stopped due to a northward turning in the IMF and the subsequent decay of the polar cap patch ionization due to recombination. This means that there is not more than a 15 min memory in the polar cap flow system, a time scale which is short compared to the ~1–3 h transit time of patches across the polar cap. Freeing our mind from the classical twin-cell picture plasma flow, to the dynamic flow picture driven by transient reconnection, there exists therefore no reason that patches obey loyalty to any one convection cell. Indeed, *Hosokawa et al*. [2010a] documented patch splitting due to reconfiguration of plasma convection.

Let us now consider a possible scenario when patches are pulled across the polar cap boundary, out of the polar cap around magnetic midnight. Figure 8c illustrates patch grabbing by transient tail reconnection. On the nightside the polar cap boundary leaps poleward into the polar cap in response to tail reconnection, grabs a patch or a part of a patch, due to the twin-cell flow disturbance generated by the reconnection pulse. The poleward auroral boundary can be used as a proxy for the OCB, and in Figure 3 it can be seen that it leaps

poleward to grab patches. From the movie we see several clear examples of poleward auroral boundary leaps and the movement of patches directly into this active reconnection region. Cigar-shaped patches exceeded the all-sky camera field of view. We suggest that such an elongated form may split in parts when grabbed by a tail reconnection event. This is illustrated in Figures 8c and 8d. The extent of the cut part pulled into the auroral oval is determined by the extent of the newly closed flux area. The flow disturbance expanding from the reconnecting area will split up the plasma patch in two parts: one part drifting east on the dusk cell and the other part drifting west on the dawn cell as illustrated in figure. This mechanism can explain the symmetry in patch exits around magnetic midnight.

5. Summary and Concluding Remarks

We have presented a high-resolution movie documenting in detail how 630.0 nm patches are pulled out from polar cap into the nighttime auroras caused by tail reconnection. This is the first direct monitoring of *F* region patches exiting the polar cap on both convection cells. A statistical study shows that the bell-shaped MLT distribution of patch exits centered on ~23:30 MLT which is marginally affected by the IMF B_y polarity. There is an expected IMF B_y polarity skew on the flanks of this distribution function attributable to the IMF control of the convection flow patterns. Our observations are consistent with the idea that both convection cells are populated by polar cap patches independent of the IMF B_y polarity. This also implies that patch exits occur on both convection cells simultaneously, which can be explained by the *Lockwood and Carlson*'s [1992] model for patch formation. Based on the *Cowley and Lockwood*'s [1992] transient flow model we suggest that patch forms are cut in parts by tail reconnection and then diverted toward dawn and dusk. We noticed that the patch intensity was less in the dusk cell than in the dawn cell for the case study presented. It remains to be studied whether there is a dawn-dusk gradient in patch density.

In conclusion, our observations are consistent with the existing view that intake of solar EUV-ionized plasma into the polar cap around magnetic noon occurs for both IMF B_y polarities [*Moen et al*., 2008], and we have provided a possible explanation for how polar cap patch material exiting the polar cap around midnight can occur on both convection cells, as earlier reported by *Crowley et al*. [2000], *Moen et al*. [2007], and *Bust and Crowley* [2007]. Patches are subject to the gradient drift instability giving rise to scintillations of Global Navigation Satellite Systems signals, and the complexity of transient polar cap flows needs to be resolved when trying to develop space weather models for the polar cap ionosphere. The MLT statistics presented on polar cap exits has practical implications for future radio wave scintillation forecasts. When the 630.0 nm polar cap patches disappear into the nighttime auroral oval they change status to auroral blobs [*Crowley et al*., 2000]. *Jin et al*. [2014] recently documented that the scintillation level increases as the patch crosses the OCB into the auroral oval, and the results presented here may be a useful element of future scintillation forecasts.

Acknowledgments

Thanks to the Norwegian Polar Institute for hosting the University of Oslo's optical instrumentation at Ny-Ålesund, Svalbard. The ground optical data used in this paper can be provided on request to Bjørn Lybekk (bjorn.lybekk@fys.uio.no), who is in charge of the optical database at the University of Oslo. The solar wind data from the ACE spacecraft can be accessed through the ACE science center at http://www.srl.caltech.edu/ACE/ASC/. The global image of aurora from the IMAGE spacecraft used in this paper can be provided on request to Harald Frey (hfrey@ssl.berkeley.edu). The TEC data were downloaded through the Madrigal database at Haystack Observatory. The authors acknowledge the use of SuperDARN data. SuperDARN is a collection of radars funded by national scientific funding agencies of Australia, Canada, China, France, Japan, South Africa, United Kingdom, and the United States of America. This project has been sponsored by the Research Council of Norway grant 208006. This research is a part of the 4DSpace initiative at the University of Oslo.

Alan Rodger thanks John Ruohoniemi and another reviewer for their assistance in evaluating this paper.

References

Anderson, D. N., J. Buchau, and R. A. Heelis (1988), Origin of density enhancements in the winter polar cap ionosphere, *Radio Sci.*, *23*, 513–519, doi:10.1029/RS023i004p00513.

Basu, S., E. MacKenzie, S. Basu, W. R. Coley, J. R. Sharber, and W. R. Hoegy (1990), Plasma structuring by the gradient drift instability at high latitudes and comparison with velocity shear driven processes, *J. Geophys. Res.*, *95*, 7799–7818, doi:10.1029/JA095iA06p07799.

Blanchard, G. T., L. R. Lyons, O. de la Beaujardière, R. A. Doe, and M. Mendillo (1996), Measurement of the magnetotail reconnection rate, *J. Geophys. Res.*, *101*, 15,265–15,276, doi:10.1029/96JA00414.

Buchau, J., B. W. Reinisch, E. J. Weber, and J. G. Moore (1983), Structure and dynamics of the winter polar cap *F* region, *Radio Sci.*, *18*, 995–1010, doi:10.1029/RS018i006p00995.

Bust, G. S., and G. Crowley (2007), Tracking of polar cap ionospheric patches using data assimilation, *J. Geophys. Res.*, *112*, A05307, doi:10.1029/2005JA011597.

Cannon, P. S., B. W. Reinisch, T. W. Bullett, and J. Buchau (1991), Response of the polar cap *F* region convection direction to changes in the interplanetary magnetic field: Digisonde measurements in northern Greenland, *J. Geophys. Res.*, *96*, 1239–1250, doi:10.1029/90JA02128.

Carlson, H. C. (2003), A voyage of discovery into the polar cap and Svalbard, in *Proceedings of the Egeland Symposium on Auroral and Atmospheric Research*, edited by J. Moen and J. A. Holtet, pp. 33–54, Dep. of Physics, Univ. of Oslo, Norway.

Carlson, H. C., K. Oksavik, J. Moen, and T. Pedersen (2004), Ionospheric patch formation: Direct measurements of the origin of a polar cap patch, *Geophys. Res. Lett.*, *31*, L08806, doi:10.1029/2003GL018166.

Carlson, H. C., T. Pedersen, S. Basu, M. Keskinen, and J. Moen (2007), Case for a new process, not mechanism, for cusp irregularity production, *J. Geophys. Res.*, *112*, A11304, doi:10.1029/2007JA012384.

Chisham, G., et al. (2007), A decade of the Super Dual Auroral Radar Network (SuperDARN): Scientific achievements, new techniques and future directions, *Surv. Geophys.*, *28*, 33–109, doi:10.1007/s10712-007-9017-8.

Chiu, M. C., et al. (1998), ACE spacecraft, *Space Sci. Rev.*, *86*, 257–284, doi:10.1023/A:1005002013459.

Coley, W. R., and R. A. Heelis (1998), Structure and occurrence of polar ionization patches, *J. Geophys. Res.*, *103*, 2201–2208, doi:10.1029/97JA03345.

Cowley, S. W. H., and M. Lockwood (1992), Excitation and decay of solar wind-driven flows in the magnetosphere-ionosphere system, *Ann. Geophys.*, *10*, 103–115.
Crowley, G. (1996), Critical review of ionospheric patches and blobs, in *The Review of Radio Science 1992–1996*, edited by W. Ross Stone, Oxford Univ. Press, U. K.
Crowley, G., A. J. Ridley, D. Deist, S. Wing, D. J. Knipp, B. A. Emery, J. Foster, R. Heelis, M. Hairston, and B. W. Reinisch (2000), Transformation of high-latitude ionospheric *F* region patches into blobs during the March 21, 1990, storm, *J. Geophys. Res.*, *105*, 5215–5230, doi:10.1029/1999JA900357.
Foster, J. C. (1984), Ionospheric signatures of magnetospheric convection, *J. Geophys. Res.*, *89*, 855–865, doi:10.1029/JA089iA02p00855.
Foster, J. C., et al. (2005), Multiradar observations of the polar tongue of ionization, *J. Geophys. Res.*, *110*, A09S31, doi:10.1029/2004JA010928.
Fukui, K., J. Buchau, and C. E. Valladares (1994), Convection of polar cap patches observed at Qaanaaq, Greenland during the winter of 1989–1990, *Radio Sci.*, *29*, 231–248, doi:10.1029/93RS01510.
Haaland, S., G. Paschmann, and B. U. Ö. Sonnerup (2006), Comment on "A new interpretation of Weimer et al.'s solar wind propagation delay technique" by Bargatze et al., *J. Geophys. Res.*, *111*, A0610, doi:10.1029/2005JA011376.
Hairston, M. R., and R. A. Heelis (1990), Model of the high-latitude ionospheric convection pattern during southward interplanetary magnetic field using DE 2 data, *J. Geophys. Res.*, *95*, 2333–2343, doi:10.1029/JA095iA03p02333.
Heppner, J. P., and N. C. Maynard (1987), Empirical high-latitude electric field models, *J. Geophys. Res.*, *92*, 4467–4489, doi:10.1029/JA092iA05p04467.
Hosokawa, K., K. Shiokawa, Y. Otsuka, A. Nakajima, T. Ogawa, and J. D. Kelly (2006), Estimating drift velocity of polar cap patches with all-sky airglow imager at Resolute Bay, Canada, *Geophys. Res. Lett.*, *33*, L15111, doi:10.1029/2006GL026916.
Hosokawa, K., K. Shiokawa, Y. Otsuka, T. Ogawa, J.-P. St-Maurice, G. J. Sofko, and D. A. Andre (2009a), Relationship between polar cap patches and field-aligned irregularities as observed with an all-sky airglow imager at Resolute Bay and the PolarDARN radar at Rankin Inlet, *J. Geophys. Res.*, *114*, A03306, doi:10.1029/2008JA013707.
Hosokawa, K., T. Kashimoto, S. Suzuki, K. Shiokawa, Y. Otsuka, and T. Ogawa (2009b), Motion of polar cap patches: A statistical study with all-sky airglow imager at Resolute Bay, Canada, *J. Geophys. Res.*, *114*, A04318, doi:10.1029/2008JA014020.
Hosokawa, K., T. Tsugawa, K. Shiokawa, Y. Otsuka, T. Ogawa, and M. R. Hairston (2009c), Unusually elongated, bright airglow plume in the polar cap *F* region: Is it a tongue of ionization?, *Geophys. Res. Lett.*, *36*, L07103, doi:10.1029/2009GL037512.
Hosokawa, K., J.-P. St-Maurice, G. J. Sofko, K. Shiokawa, Y. Otsuka, and T. Ogawa (2010a), Reorganization of polar cap patches through shears in the background plasma convection, *J. Geophys. Res.*, *115*, A01303, doi:10.1029/2009JA014599.
Hosokawa, K., T. Tsugawa, K. Shiokawa, Y. Otsuka, N. Nishitani, T. Ogawa, and M. R. Hairston (2010b), Dynamic temporal evolution of polar cap tongue of ionization during magnetic storm, *J. Geophys. Res.*, *115*, A12333, doi:10.1029/2010JA015848.
Hosokawa, K., J. I. Moen, K. Shiokawa, and Y. Otsuka (2011), Decay of polar cap patch, *J. Geophys. Res.*, *116*, A05306, doi:10.1029/2010JA016297.
Hosokawa, K., S. Taguchi, Y. Ogawa, and T. Aoki (2013), Periodicities of polar cap patches, *J. Geophys. Res. Space Physics*, *118*, 447–453, doi:10.1029/2012JA018165.
Hosokawa, K., S. Taguchi, K. Shiokawa, Y. Otsuka, Y. Ogawa, and M. Nicolls (2014), Global imaging of polar cap patches with dual airglow imagers, *Geophys. Res. Lett.*, *41*, 1–6, doi:10.1002/2013GL058748.
Jin, Y., J. I. Moen, and W. J. Miloch (2014), GPS scintillation effects associated with polar cap patches and substorm auroral activity: Direct comparison, *J. Space Weather Space Clim.*, *4*, A23, doi:10.1051/swsc/2014019.
Lockwood, M., and H. C. Carlson (1992), Production of polar cap electron density patches by transient magnetopause reconnection, *Geophys. Res. Lett.*, *19*, 1731–1734, doi:10.1029/92GL01993.
Lockwood, M., J. A. Davies, J. Moen, A. P. van Eyken, K. Oksavik, I. W. McCrea, and M. Lester (2005), Motion of the dayside polar cap boundary during substorm cycles: II. Generation of poleward-moving events and polar cap patches by pulses in the magnetopause reconnection rate, *Ann. Geophys.*, *23*, 3513–3532, doi:10.5194/angeo-23-3513-2005.
Lorentzen, D. A., N. Shumilov, and J. Moen (2004), Drifting airglow patches in relation to tail reconnection, *Geophys. Res. Lett.*, *31*, L02806, doi:10.1029/2003GL017785.
Makarevich, R. A., and M. J. Nicolls (2013), Statistical comparison of TEC derived from GPS and ISR observations at high latitudes, *Radio Sci.*, *48*, 441–452, doi:10.1002/rds.20055.
McComas, D. J., S. J. Bame, P. Barker, W. C. Feldman, J. L. Phillips, P. Riley, and J. W. Griffee (1998), Solar Wind Electron Proton Alpha Monitor (SWEPAM) for the Advanced Composition Explorer, *Space Sci. Rev.*, *86*, 563–612, doi:10.1023/A:1005040232597.
McEwen, D. J., and D. P. Harris (1996), Occurrence patterns of *F* layer patches over the north magnetic pole, *Radio Sci.*, *31*, 619–628, doi:10.1029/96RS00312.
Mende, S. B., et al. (2000a), Far ultraviolet imaging from the IMAGE spacecraft. 1. System design, *Space Sci. Rev.*, *91*, 243–270.
Mende, S. B., et al. (2000b), Far ultraviolet imaging from the IMAGE spacecraft. 2. Wideband FUV imaging, *Space Sci. Rev.*, *91*, 271–285.
Milan, S. E., M. Lester, and T. K. Yeoman (2002), HF radar polar patch formation revisited: Summer and winter variations in dayside plasma structuring, *Ann. Geophys.*, *20*, 487–499, doi:10.5194/angeo-20-487-2002.
Mitchell, C. N., L. Alfonsi, G. De Franceschi, M. Lester, V. Romano, and A. W. Wernik (2005), GPS TEC and scintillation measurements from the polar ionosphere during the October 2003 storm, *Geophys. Res. Lett.*, *32*, L12S03, doi:10.1029/2004GL021644.
Moen, J., P. E. Sandholt, M. Lockwood, W. F. Denig, U. P. Lövhaug, B. Lybekk, A. Egeland, D. Opsvik, and E. Friis-Christensen (1995), Convection events and dayside auroral activity, *J. Geophys. Res.*, *100*, 23,917–23,934, doi:10.1029/95JA02585.
Moen, J., H. C. Carlson, K. Oksavik, C. P. Nielsen, S. E. Pryse, H. R. Middleton, I. W. Mccrea, and P. Gallop (2006), EISCAT observations of plasma patches at sub-auroral cusp latitudes, *Ann. Geophys.*, *24*, 2363–2374, doi:10.5194/angeo-24-2363-2006.
Moen, J., N. Gulbrandsen, D. A. Lorentzen, and H. C. Carlson (2007), On the MLT distribution of *F* region polar cap patches at night, *Geophys. Res. Lett.*, *34*, L14113, doi:10.1029/2007GL029632.
Moen, J., X. C. Qiu, H. C. Carlson, R. Fujii, and I. W. McCrea (2008), On the diurnal variability in F_2-region plasma density above the EISCAT Svalbard radar, *Ann. Geophys.*, *26*, 2427–2433, doi:10.5194/angeo-26-2427-2008.
Moen, J., K. Oksavik, L. Alfonsi, Y. Daabakk, V. Romano, and L. Spogli (2013), Space weather challenges of the polar cap ionosphere, *J. Space Weather Space Clim.*, *3*, A02, doi:10.1051/swsc/2013025.
Ober, D. M., N. C. Maynard, W. J. Burke, W. K. Peterson, J. B. Sigwarth, L. A. Frank, J. D. Scudder, W. J. Hughes, and C. T. Russell (2001), Electrodynamics of the poleward auroral border observed by Polar during a substorm on April 22, 1998, *J. Geophys. Res.*, *106*, 5927–5944, doi:10.1029/2000JA003024.
Oksavik, K., V. L. Barth, J. Moen, and M. Lester (2010), On the entry and transit of high-density plasma across the polar cap, *J. Geophys. Res.*, *115*, A12308, doi:10.1029/2010JA015817.

Østgaard, N., J. Moen, S. B. Mende, H. U. Frey, T. J. Immel, P. Gallop, K. Oksavik, and M. Fujimoto (2005), Estimates of magnetotail reconnection rate based on IMAGE FUV and EISCAT measurements, *Ann. Geophys.*, *23*, 123–134, doi:10.5194/angeo-23-123-2005.

Pedersen, T. R., B. G. Fejer, R. A. Doe, and E. J. Weber (2000), An incoherent scatter radar technique for determining two-dimensional horizontal ionization structure in polar cap *F* region patches, *J. Geophys. Res.*, *105*, 10,637–10,656, doi:10.1029/1999JA000073.

Pitout, F., and P.-L. Blelly (2003), Electron density in the cusp ionosphere: Increase or depletion?, *Geophys. Res. Lett.*, *30*(14), 1726, doi:10.1029/2003GL017151.

Pitout, F., C. Escoubet, and E. Lucek (2004), Ionospheric plasma density structures associated with magnetopause motion: A case study using the Cluster spacecraft and the EISCAT Svalbard radar, *Ann. Geophys.*, *22*, 2369–2379, doi:10.5194/angeo-22-2369-2004.

Prikryl, P., P. T. Jayachandran, S. C. Mushini, D. Pokhotelov, J. W. MacDougall, E. Donovan, E. Spanswick, and J.-P. St.-Maurice (2010), GPS TEC, scintillation and cycle slips observed at high latitudes during solar minimum, *Ann. Geophys.*, *28*, 1307–1316, doi:10.5194/anngeo-28-1307-2010.

Prikryl, P., P. T. Jayachandran, S. C. Mushini, and R. Chadwick (2011), Climatology of GPS phase scintillation and HF radar backscatter for the high-latitude ionosphere under solar minimum conditions, *Ann. Geophys.*, *29*, 377–392, doi:10.5194/angeo-29-377-2011.

Rideout, W., and A. Coster (2006), Automated GPS processing for global total electron content data, in *GPS Solutions*, vol. 10, pp. 219–228, Springer, Berlin, doi:10.1007/s10291-006-0029-5.

Robinson, R. M., R. T. Tsunoda, J. F. Vickrey, and L. Guerin (1985), Sources of *F* region ionization enhancements in the nighttime auroral zone, *J. Geophys. Res.*, *90*, 7533–7546, doi:10.1029/JA090iA08p07533.

Rodger, A. S., M. Pinnock, J. R. Dudeney, J. Waterman, O. de La Beaujardiere, and K. B. Baker (1994), Simultaneous two hemisphere observations of the presence of polar patches in the nightside ionosphere, *Ann. Geophys.*, *12*, 642–648, doi:10.1007/s00585-994-0642-y.

Ruohoniemi, J. M., and K. B. Baker (1998), Large-scale imaging of high-latitude convection with Super Dual Auroral Radar Network HF radar observations, *J. Geophys. Res.*, *103*, 20,797–20,811, doi:10.1029/98JA01288.

Ruohoniemi, J. M., and R. A. Greenwald (1996), Statistical patterns of high-latitude convection obtained from Goose Bay HF radar observations, *J. Geophys. Res.*, *101*, 21,743–21,764, doi:10.1029/96JA01584.

Ruohoniemi, J. M., and R. A. Greenwald (2005), Dependencies of high-latitude plasma convection: Consideration of interplanetary magnetic field, seasonal, and universal time factors in statistical patterns, *J. Geophys. Res.*, *110*, A09204, doi:10.1029/2004JA010815.

Sakai, J., S. Taguchi, K. Hosokawa, and Y. Ogawa (2013), Steep plasma depletion in dayside polar cap during a CME-driven magnetic storm, *J. Geophys. Res. Space Physics*, *118*, 462–471, doi:10.1029/2012JA018138.

Siscoe, G. L., and T. S. Huang (1985), Polar cap inflation and deflation, *J. Geophys. Res.*, *90*, 543–547, doi:10.1029/JA090iA01p00543.

Smith, C. W., J. L'Heureux, N. F. Ness, M. H. Acuña, L. F. Burlaga, and J. Scheifele (1998), The ACE magnetic fields experiment, *Space Sci. Rev.*, *86*, 613–632, doi:10.1023/A:1005092216668.

Sojka, J. J., M. D. Bowline, R. W. Schunk, D. T. Decker, C. E. Valladares, R. Sheehan, D. N. Anderson, and R. A. Heelis (1993), Modeling polar cap *F*-region patches using time varying convection, *Geophys. Res. Lett.*, *20*, 1783–1786, doi:10.1029/93GL01347.

Sonnerup, B. U. Ö., and M. Scheible (1998), Minimum and maximum variance analysis, in *Analysis Methods for Multi-Spacecraft Data*, ISSI Sci. Rep. Ser., vol. 1, edited by G. Paschmann and P. Daly, pp. 185–220.

Spogli, L., L. Alfonsi, G. De Franceschi, V. Romano, M. H. O. Aquino, and A. Dodson (2009), Climatology of GPS ionospheric scintillations over high and mid-latitude European regions, *Ann. Geophys.*, *27*, 3429–3437, doi:10.5194/angeo-27-3429-2009.

Valladares, C. E., S. Basu, J. Buchau, and E. Friis-Christensen (1994), Experimental evidence for the formation and entry of patches into the polar cap, *Radio Sci.*, *29*, 167–194, doi:10.1029/93RS01579.

Weber, E. J., J. Buchau, J. G. Moore, J. R. Sharber, R. C. Livingston, J. D. Winningham, and B. W. Reinisch (1984), *F* layer ionization patches in the polar cap, *J. Geophys. Res.*, *89*, 1683–1694, doi:10.1029/JA089iA03p01683.

Weimer, D. R. (1995), Models of high-latitude electric potentials derived with a least error fit of spherical harmonic coefficients, *J. Geophys. Res.*, *100*, 19,595–19,608, doi:10.1029/95JA01755.

Weimer, D. R., and J. H. King (2008), Improved calculations of interplanetary magnetic field phase front angles and propagation time delays, *J. Geophys. Res.*, *113*, A01105, doi:10.1029/2007JA012452.

Wood, A. G., S. E. Pryse, and J. Moen (2009), Modulation of nightside polar patches by substorm activity, *Ann. Geophys.*, *27*, 3923–3932, doi:10.5194/angeo-27-3923-2009.

Zhang, Q.-H., et al. (2011), On the importance of interplanetary magnetic field B_y on polar cap patch formation, *J. Geophys. Res.*, *116*, A05308, doi:10.1029/2010JA016287.

Zhang, Q.-H., et al. (2013a), Direct observations of the evolution of polar cap ionization patches, *Science*, *339*, 1597–1600, doi:10.1126/science.1231487.

Zhang, Q.-H., B.-C. Zhang, J. Moen, M. Lockwood, I. W. McCrea, H.-G. Yang, H.-Q. Hu, R.-Y. Liu, S.-R. Zhang, and M. Lester (2013b), Polar cap patch segmentation of the tongue of ionization in the morning convection cell, *Geophys. Res. Lett.*, *40*, 2918–2922, doi:10.1002/grl.50616.

Zhang, Y., D. J. McEwen, and L. L. Cogger (2003), Interplanetary magnetic field control of polar patch velocity, *J. Geophys. Res.*, *108*(A5), 1214, doi:10.1029/2002JA009742.